

# Effect of Al<sub>2</sub>O<sub>3</sub> Content and Process Variables on Structure and Properties of Al-Al<sub>2</sub>O<sub>3</sub> Compacts

Arindam Ghosh<sup>1,2</sup>, Subrata Chatterjee<sup>1</sup>

<sup>1</sup>Department of Metallurgy and Materials Engineering, Bengal Engineering and Science University, Howrah, India

<sup>2</sup>Presently at National Engineering Industries Ltd., Jaipur, India

Email: [ghosh.arind@gmail.com](mailto:ghosh.arind@gmail.com)

Received 1 November 2013; revised 10 December 2013; accepted 30 December 2013

Copyright © 2014 by authors and Scientific Research Publishing Inc.

This work is licensed under the Creative Commons Attribution International License (CC BY).

<http://creativecommons.org/licenses/by/4.0/>



Open Access

---

## Abstract

Aluminium-alumina compacts with varying wt% of alumina were compacted in the pressure range of 115 - 290 MPa. Compacts prepared at 290 MPa pressure, were sintered in an argon atmosphere at 573, 673, 773 and 873 K for 1 hour. The green density, % porosity, % spring back and hardness of the green compacts were determined. Scanning Electron Microscopy was carried out to observe the morphology of pores and alumina particles in green and sintered compacts. The present study indicates that, densification of the compact increases with increasing compacting pressure and decreases with increasing alumina content. Maximum density achieved is 93% for pure aluminium compacts and decreases to 85% for Al-20 wt% alumina compacts. Grain growth of aluminium particles is noticed in the compacts after sintering at 773 and 873 K. Dispersion of fine alumina particle in the aluminium matrix occurs predominantly in the compact when sintered at 773 K which results in increase in hardness value.

## Keywords

Al-Al<sub>2</sub>O<sub>3</sub> Compacts; Porosity; Spring Back; Residual Stress; Sintering

---

## 1. Introduction

The increasing demand for strong light Al-alloys by the aerospace, defence and housing industries has been a persistent pressure on the development of alloys with superior mechanical properties. In addition to alloying, reinforcing the alloy with fibers, whiskers and particulates has been made since 1960 [1]-[3]. Much of these

composites have been commercialized for various applications [4] [5]. Among the many Al-reinforced composites, reinforcing aluminium by alumina particles has been the most popular [6]-[9]. However, the poor wettability of alumina particles causes a severe problem in producing these composites by conventional melting and casting technique [10]. This problem can be overcome to many extents by additions of MgO, Mg ribbon or magnesium coated alumina [11]-[13]. This of course makes the system more complex with a high intricacy of the production technique. The adoption of powder metallurgy technique of blending, pressing and sintering in preparing such composites has become a convenient and cost-effective route to produce such composites [14]-[16]. Hence, compaction and sintering behaviour of Al-Al<sub>2</sub>O<sub>3</sub> compacts has become a subject of interest for a quite long time. In the present study, efforts have been given to characterize compaction and sintering behavior of aluminium-alumina compacts at different process variables.

## 2. Experimental

The shape, size and morphology of aluminium and alumina powders were observed in scanning electron microscope (SEM) at different magnifications and the sieve analysis was carried out. The tap density and apparent density of the powders were measured. Aluminium powders of -300 mesh size and alumina powders of -350 mesh were mixed in a ball mill of 1 Kg capacity. The mixed powders were pressed at various pressures from 115 MPa to 290 MPa in a pneumatic press of 25.4 mm die. The density, % porosity, hardness and % spring back of the green compacts were determined. The green compacts of height/diameter (h/D) ratio ~0.25 compressed at 290 MPa were sintered at various temperature like 573, 673, 773 and 873 K for one hour in an argon atmosphere. The density, % porosity, % volume change and hardness values of the sintered compacts were evaluated as a function of sintering temperature. Extensive microstructural characterization was done using SEM.

## 3. Results and Discussions

### 3.1. Characterization of Powder Particles

SEM analysis shows (Figure 1(a)) size of the aluminium particles lies within 3 - 18 micron. Alumina particles are comparatively smaller in size and the range lies between 0.4 to 4 microns (Figure 1(b)).

Most of the alumina particles are angular and some of them are spherical. Figure 2 shows the tap density and apparent density of the aluminium and alumina powders. For aluminium particles, increase in tap density w.r.t. apparent density is 53% whereas for alumina particle it is only 22% due to uniform smaller particle size.

### 3.2. Compaction Behaviour of Aluminium and Aluminium-Alumina Compacts

Figure 3 shows the densification parameter of aluminium and Al-Al<sub>2</sub>O<sub>3</sub> compacts at different compacting pressures. The densification curves (in Figure 3) have been divided into three segments. Generally in a uniaxial press densification of pure metal powder is achieved through three different stages.

At the initial stage of compaction, powder particles come together and the contact regions increase with in-

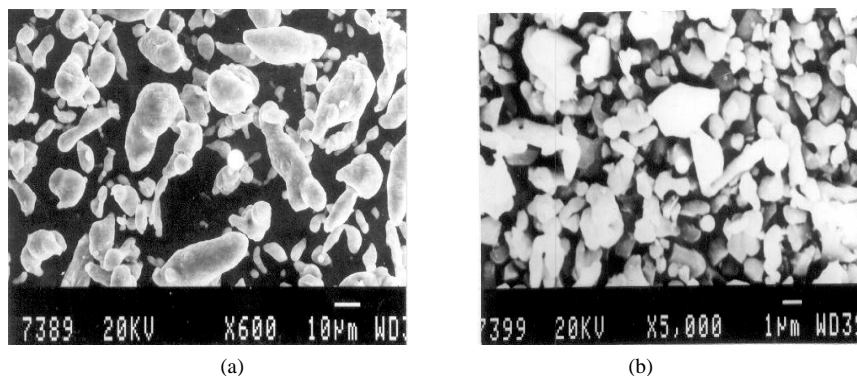
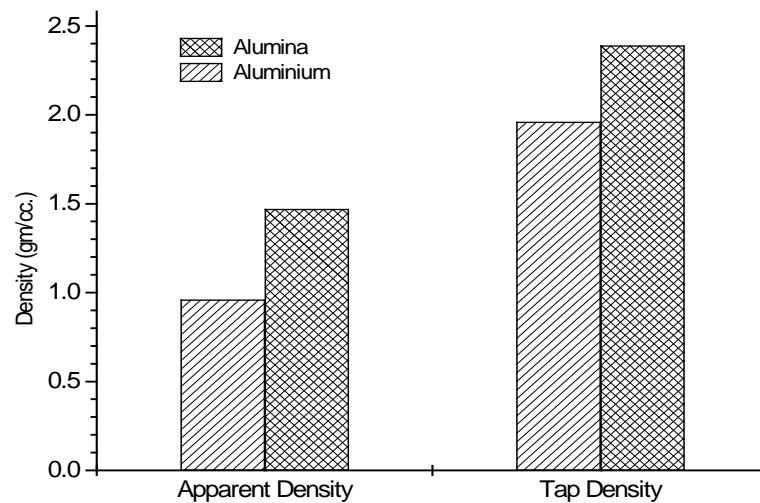
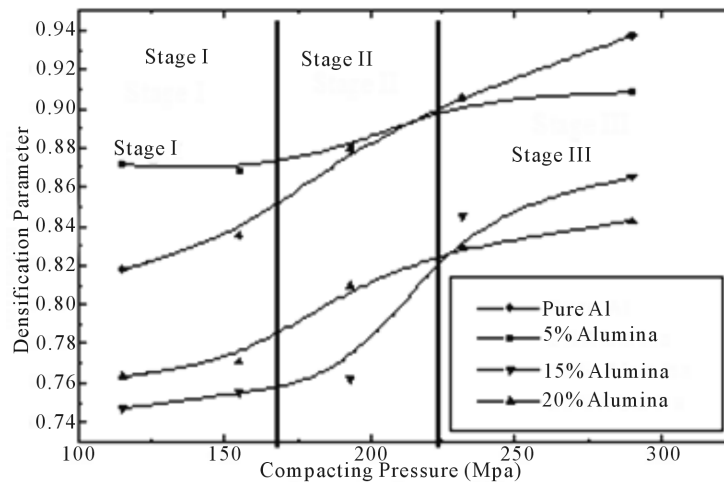


Figure 1. Exhibits size, morphology and shape of powder particles. (a) Aluminium powder; (b) Alumina particles.



**Figure 2** Apparent density and tap density of aluminium and alumina powders.



**Figure 3.** Densification parameter is plotted as a function of compacting pressure.

crease in compressive load. The rate of increase in densification parameter is very slow at this stage (stage 1 in **Figure 3**). In the next stage the outer oxide layer of metal powder (which is generally harder than the base metal) breaks off and the contact areas rapidly increase through flattening of metal powder. The densification rate is faster at this condition (stage II). Finally a plateau region is reached beyond which densification remains almost same with further increase in compacting pressure (stage III). For pure aluminium powder compact, an extent of 93% densification has been achieved at 290 MPa compressive load. This is achieved by a high amount of plastic deformation of aluminium particle which in turn fill up the holes and the triple point by material flow (**Figure 4(a)**). At this high compressive load maximum flattening of powder particles occur and complete cold welding between the particles is observed (**Figure 4(b)**). By introducing varying amount of alumina particle into aluminium powder the compaction characteristics of Al-alumina compact behaves differently. It is interesting to observe from **Figure 3** that by adding only 5 wt% alumina better densification (of maximum 90%) has been obtained as finer size  $\text{Al}_2\text{O}_3$  particles occupy the voids created by larger aluminium particles where as with increase in alumina content the densification parameter drops to 85% for Al-20 wt% alumina compact at 290 MPa compacting pressure. This has been explained by the scanning electron micrographs of **Figure 5**. **Figure 5** shows Al-20 wt% alumina green compact where a very fine alumina of 100 nm size has been identified between two aluminium particles and a portion of the hard angular alumina particles has been embedded into soft

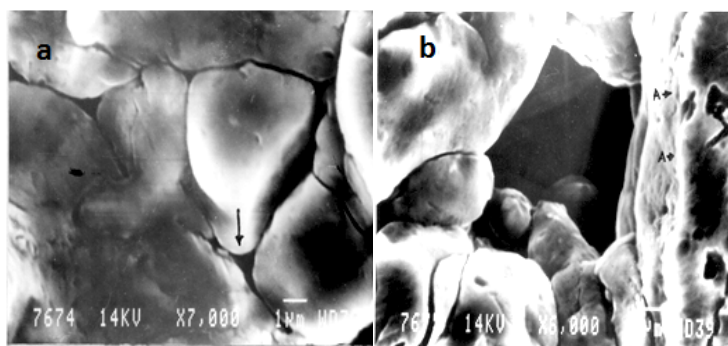


**Figure 4.** Micrograph of pure aluminium powder green compact compressed at 290 MPa. (a) Pores are filled up by deformed aluminium as indicated; (b) Individual aluminium particle has been cold welded in the region marked A.

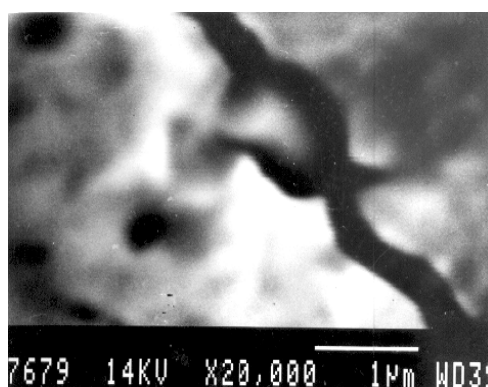


**Figure 5.** A hair line separation by a small alumina particulate (~300 nm) between two aluminium particles.

ductile aluminium matrix. This tiny alumina particle acts as a barrier for cold welding of aluminium particles. The increase in alumina content results in a loss of densification in the green compact.

This is further confirmed by measuring the inter separation distance of aluminium particles in different compacts. In Al-5 wt% alumina compact this was measured as low as 100 nm and can be identified as thin black line between the particles (**Figure 6(a)**). The inter separation distance become more pronounced when alumina content is increased up to 15% and the inter separation distance increases up to 4  $\mu\text{m}$  (**Figure 6(b)**). This low densification at higher alumina content obviously leads to generate a greater amount of porosity and loss of green strength in the compact. **Figure 7** shows the variation of green hardness as a function of alumina content at various compacting pressure. It is observed from the **Figure 7** that a sharp fall in green hardness of the Al-Al<sub>2</sub>O<sub>3</sub> compact has occurred beyond 15 wt% alumina content at high compacting pressure of 290 MPa. For low compacting pressure (115 - 193 MPa) this sharp fall in hardness has occurred after 5 wt% alumina content.

Spring back of the green compacts was calculated just after removal of compressive load and ejection of the compacts from mould. % Spring back was found to increase with increased alumina reinforcement and compressive load. **Figure 8** shows the % spring back of green compacts as a function of alumina content at various compressive pressures. Increased amount of Alumina has resulted in greater amount of elastic recovery, which ultimately gives higher spring back value for high alumina content system. Greater amount of elastic recovery has also occurred even at comparatively high compressive pressure. But the % of alumina content has become the predominant factor for higher spring back of the green compact.

### 3.3. Characterisation of Sintered Compact

The most essential feature in sintering is the annihilation of vacant space in a porous powder compact and thus a

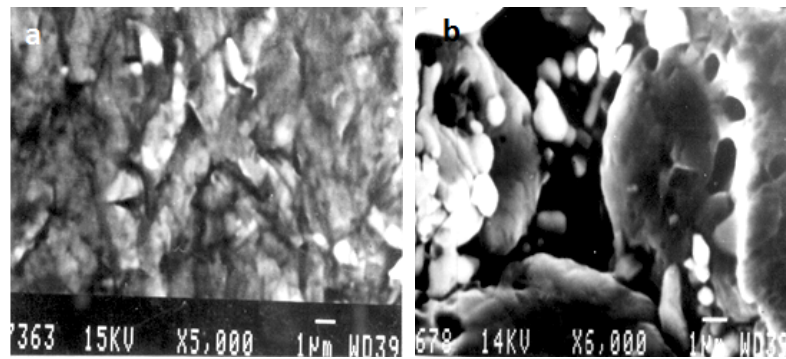


**Figure 6.** (a) Aluminium 5 wt% alumina green compact compressed at 290 MPa. Inter separation distance between aluminium powders is less than 100  $\mu\text{m}$ ; (b) Aluminium 15 wt% alumina green compact compressed at 290 MPa. Inter separation distance has increased to 4  $\mu\text{m}$ .

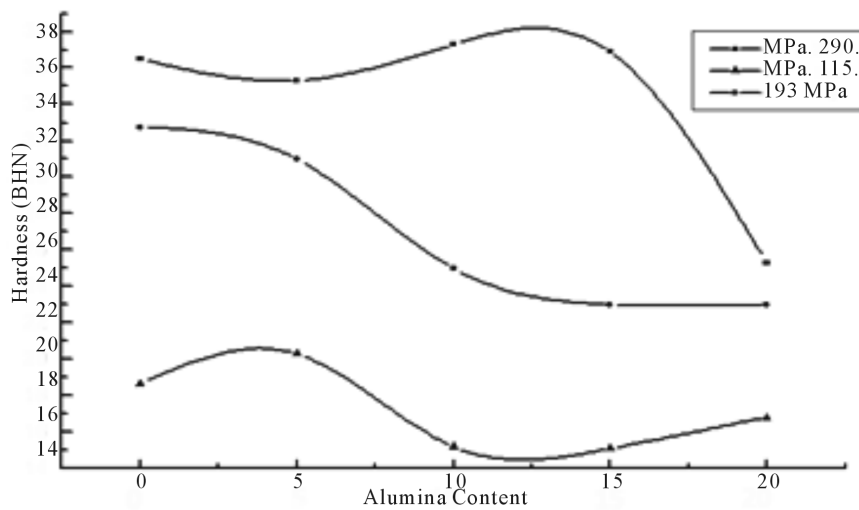


**Figure 7.** Effect of alumina content on hardness of green compacts at different compacting pressure.

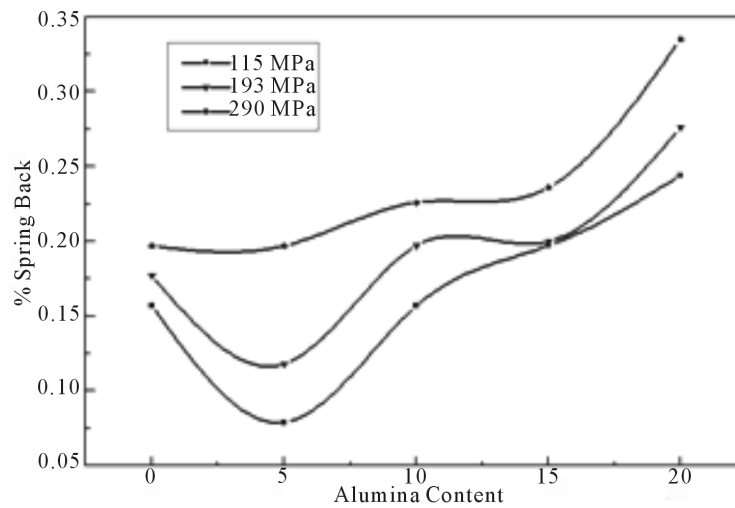


**Figure 8.** Exhibits % spring back as a function of alumina content at different compacting pressure.

decrease in percent porosity is expected to occur on sintering. **Figure 9** shows a change in % porosity of the Al-alumina compacts at various sintering temperatures. It is observed for Al-5 wt% alumina compact that initial 10% porosity in green compact has dropped to 4% on sintering at 673 K.

At higher sintering temperature of 873 K, an increase in % porosity indicates a volume expansion due to the expansion of entrapped gases in the compact. Same trend has also been observed for Al-10 wt% alumina and Al-15 wt% alumina compacts. Another objective of sintering is to strengthen the powder compact by solid state bonding between the powder particles. The variation in hardness of the sintered compact at different sintering temperatures is shown in **Figure 10**.

It is interesting to note that a decreasing trend in hardness value has been noticed with increase in sintering temperature. It is then obvious that softening of strain hardened aluminium particles occurs as the sintering temperature gradually increases though the solid state bonding between the particles was observed at 573 K temperature (**Figure 11**) but the softening of aluminium over balanced the bonding strength which occur during sintering.

It is somehow intriguing to observe that a sudden increase in hardness of Al-15 wt% and Al-10 wt% alumina

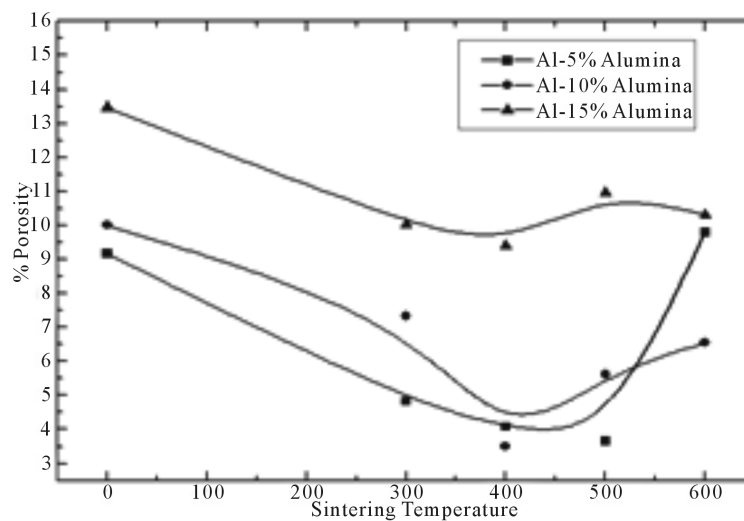


**Figure 9.** Effect of sintering temperature on % porosity of the compacts.

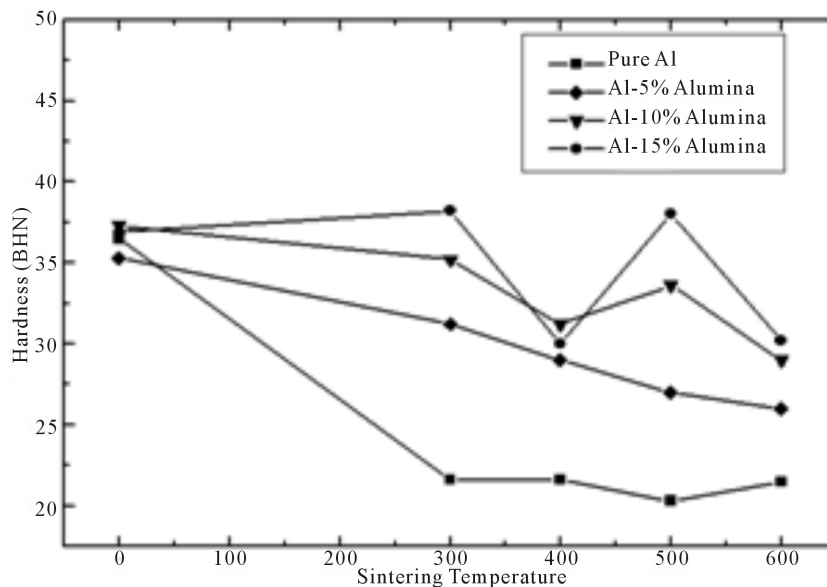


**Figure 10.** Effect of sintering temperature on hardness of the compacts.

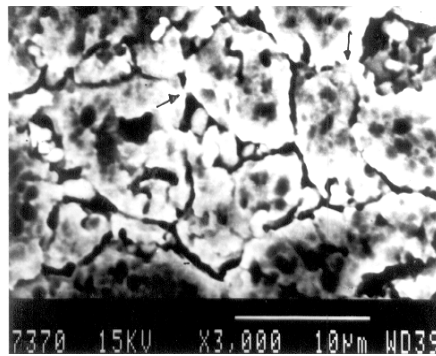


**Figure 11.** Aluminium 15 wt% alumina compact sintered at 573 K shows bonding between aluminium particles have occurred (indicated by arrows) as a result of sintering.

compact on sintering at 773 K. Again at 873 K sintering temperature, grain growth of Al particles lower the hardness of the compacts (**Figure 10**).

#### 4. Conclusions

Densification parameters increase with the increase in compacting pressure. 93% of densification can be achieved for pure Al-compacts, which decreases to 85% for Al-20 wt%  $\text{Al}_2\text{O}_3$  compacts at 290 MPa pressure.

% Spring back is increased if the alumina content as well as compacting pressure is increased.

On sintering, hardness of the sintered compact gradually decreases with increasing temperature. At 773 K sintering temperature, a sudden increase in hardness was observed for Al-10 wt% and Al-15 wt%. Alumina compacts due to uniform distribution of fine alumina particles in aluminium matrix.

#### Acknowledgements

Authors gratefully acknowledge Central Glass and Ceramic Research Institute (CGCRI), Jadavpur, West Bengal India and Dr. Swapan Kumar Das, National Metallurgical Laboratory, Jamshedpur India for their support to carry out some of the experimental works in this research paper.

#### References

- [1] Ibrahim, I.A., Mohamed, F.A. and Lavernia, E.J. (1991) Particulate Reinforced Metal Matrix Composites—A Review. *Journal of Material Science*, **26**, 1137-1156. <http://dx.doi.org/10.1007/BF00544448>
- [2] Divecha, A.P., Fishman, S.G. and Karmarkar, S.D. (1981) Silicon Carbide Reinforced Aluminium—A Formable Composite. *JOM*, **33**, 12-17. <http://dx.doi.org/10.1007/BF03339487>
- [3] Kim, Y.A., Hayashi, T., Endo, M., Gotoh, Y. and Wada, N. (2006) Fabrication of Aligned Carbon Nano Tube-Filled Rubber Composite. *Scripta Materialia*, **54**, 31-35. <http://dx.doi.org/10.1016/j.scriptamat.2005.09.014>
- [4] Nutt, S.R. (1984) Defects in Silicon Carbide Whiskers. *Journal of the American Ceramic Society*, **67**, 428-431. <http://dx.doi.org/10.1111/j.1151-2916.1984.tb19730.x>
- [5] Chou, T.W., Kelly, A. and Okura, A. (1986) Fibre-Reinforced Metal-Matrix Composites. *Composites*, **16**, 187. [http://dx.doi.org/10.1016/0010-4361\(85\)90603-2](http://dx.doi.org/10.1016/0010-4361(85)90603-2)
- [6] Soma Raju, K., Bhanu Prasad, V.V., Rudrakshi, G.B. and Ojha, S.N. (2013) PM Processing of Al- $\text{Al}_2\text{O}_3$  Composites and Their Characterisation. *Materials Science Forum*, **736**, 81-97.
- [7] Srivastava, M.K., Mandal, R.K., Mohan, S., Pathak, J.P. and Ojha, S.N. (1999) Wear Characteristics of Al- $\text{Al}_2\text{O}_3$  Composites Produced by Powder Metallurgy Process. *Indian Journal of Engineering and Materials Sciences*, **6**, 27-33.
- [8] Jiang, G., Daehn, G.S. and Wagoner, R.H. (2003) Observations on Densification of Al- $\text{Al}_2\text{O}_3$  Composite Powder Compacts by Pressure Cycling. *Powder Metallurgy*, **46**, 219-223. <http://dx.doi.org/10.1179/003258903225010505>
- [9] Jiang, G., Daehn, G.S. and Wagoner, R.H. (2001) Inclusion Particle Size Effects on the Cyclic Compaction of Powder Composites. *Scripta Materialia*, **44**, 1117-1123. [http://dx.doi.org/10.1016/S1359-6462\(01\)00659-5](http://dx.doi.org/10.1016/S1359-6462(01)00659-5)

- [10] Schultz, B.F., Ferguson, J.B. and Rohatgi, P.K. (2011) Microstructure and Hardness of Al<sub>2</sub>O<sub>3</sub> Nanoparticle Reinforced Al-Mg Composites Fabricated by Reactive Wetting and Stir Mixing. *Materials Science and Engineering A*, **530**, 87-97. <http://dx.doi.org/10.1016/j.msea.2011.09.042>
- [11] Abdul-Lattef, N.I., Khedar, A.R.I. and Goel, S.K. (1985) Preparation of Al-Al<sub>2</sub>O<sub>3</sub>-MgO Cast Particulate Composites Using MgO Coating Technique. *Journal of Materials Science Letters*, **4**, 385-388. <http://dx.doi.org/10.1007/BF00719724>
- [12] Mortimer, D.A. and Nicholas, M. (1970) Wetting of Carbon by Copper and Copper Alloys. *Journal of Materials Science*, **5**, 149. <http://dx.doi.org/10.1007/BF00554633>
- [13] Kimura, Y., Mishima, Y., Umekawa, S. and Suzuki, T. (1984) Compatibility between Carbon Fiber and Binary Aluminum Alloys. *Journal of Materials Science*, **19**, 3107. <http://dx.doi.org/10.1007/BF01026990>
- [14] Akhlaghi, F. and Zare-Bidaki, A. (2009) Influence of Graphite Content on the Dry Sliding and Oil Impregnated Sliding Wear Behavior of Al 2024-Graphite Composites Produced by *in Situ* Powder Metallurgy Method. *Wear*, **266**, 37-45. <http://dx.doi.org/10.1016/j.wear.2008.05.013>
- [15] Rohatgi, P.K., Gou, R. and Keshavaram, B.N. (1995) Cast Aluminum, Fly Ash Composites for Engineering Applications. *AFS Transactions*, **103**, 575.
- [16] Ray, S. (1993) Synthesis of Cast Metal Matrix Particulate Composites. *Journal of Material Science*, **28**, 5397-5413. <http://dx.doi.org/10.1007/BF00367809>